The Interplay between Alterations in Esophageal Microbiota Associated with Th17 Immune Response and Impaired LC20 Phosphorylation in Achalasia

池田, 浩子

The Interplay between Alterations in Esophageal Microbiota Associated with Th17 Immune Response and Impaired LC20 Phosphorylation in Achalasia

Short title: Microbiota linked to Achalasia

Hiroko Ikeda[1], Eikichi Ihara[1]*, Kosuke Takeya[2], Koji Mukai[1], Manabu Onimaru[3], Kenoki Ouchida[4], Yoshitaka Hata[1], Xiaopeng Bai[1], Yoshimasa Tanaka[1], Taisuke Sasaki[5], Fumiyo Saito[2], Masumi Eto[2], Jiro Nakayama[6], Yoshinao Oda[5], Masafumi Nakamura[4], Haruhiro Inoue[3], and Yoshihiro Ogawa[1]

[1]Department of Medicine and Bioregulatory Science, Graduate School of Medical Sciences, Kyushu University, Fukuoka, Japan

[2]Faculty of Veterinary Medicine, Okayama University of Science, Ehime, Japan

[3]Digestive Diseases Center, Showa University Koto Toyosu Hospital, Tokyo, Japan

[4]Department of Surgery and Oncology, Graduate School of Medical Sciences, Kyushu University, Fukuoka, Japan

[5]Department of Anatomic Pathology, Graduate School of Medical Sciences, Kyushu University, Fukuoka, Japan

[6]Laboratory of Microbial Technology, Division of Systems Bioengineering, Department of Bioscience and Biotechnology, Faculty of Agriculture, Graduate School, Kyushu University, Fukuoka, Japan

Correspondence:

Eikichi Ihara M.D., Ph.D.

Department of Medicine and Bioregulatory Science, Graduate School of Medical Sciences, Kyushu University

3-1-1 Maidashi, Higashi-ku, Fukuoka-shi, Fukuoka 812-8582, Japan

E-mail: ihara.eikichi.167@m.kyushu-u.ac.jp

Telephone: +81-92-642-5286 Fax +81-92-642-5287

Author contributions:

Conceptualization: Hiroko Ikeda, Eikichi Ihara, Kosuke Takeya, Koji Mukai, and Manabu Onimaru; Methodology: Hiroko Ikeda, Eikichi Ihara, Kosuke Takeya, Kenoki Ouchida, Yoshitaka Hata, Taisuke Sasaki, Fumio Saito, Masumi Eto, Jiro Nakayama, and Yoshinao Oda; Formal analysis and investigation: Hiroko Ikeda, Kosuke Takeya, Koji Mukai, Xiaopeng Bai, Yoshimasa Tanaka, Taisuke Sasaki, Fumio Saito, and Masumi Eto; Writing-original draft preparation: Hiroko Ikeda, Eikichi Ihara, and Kosuke Takeya; Writing-review and editing: Masumi Eto, Jiro Nakayama, Yoshinao Oda, Masafumi Nakamura, Haruhiro Inoue, and Yoshihiro Ogawa; Funding acquisition: Eikichi Ihara and Yoshihiro Ogawa; Resources: Eikichi Ihara and Yoshihiro Ogawa; Supervision: Haruhiro Inoue and Yoshihiro Ogawa. All authors have read and approved the final manuscript.

Word count: 5104 words

Abstract

Background:

Achalasia is an esophageal motility disorder with an unknown etiology. We aimed to determine the pathogenesis of achalasia by studying alterations in esophageal smooth muscle contraction and the associated inflammatory response, and evaluate the role of esophageal microbiota in achalasia development.

Methods:

We analyzed esophageal mucosa and lower esophageal sphincter (LES) samples, obtained from patients with type II achalasia who underwent peroral endoscopic myotomy. Esophageal conditioned media obtained from patients were transferred into the mouse esophagus to determine whether the esophageal intraluminal environment is associated with achalasia.

Results:

Approximately 30% of 20-kDa myosin light chains (LC_{20}) was phosphorylated in LES from the control group under resting and stimulated conditions, whereas less than 10% of LC_{20} phosphorylation was detected in achalasia under all conditions. The hypophosphorylation of LC_{20} in achalasia was associated with the downregulation of the myosin phosphatase-inhibitor protein CPI-17. Th17-related cytokines, including IL-17A, IL-17F, IL-22, and IL-23A, were significantly upregulated in achalasia. α-Diversity index of esophageal microbiota and the proportion of several microbes, including *Actinomyces* and *Dialister*, increased in achalasia. *Actinomyces* levels positively correlated with IL-23A levels, whereas *Dialister* levels were positively associated with IL-17A, IL-17F, and IL-22 levels. Esophageal IL-17F levels increased in mice after oral administration of the conditioned media.

Conclusions:

In LES of patients with achalasia, hypophosphorylation of LC_{20}, a possible cause of impaired contractility, was associated with CPI-17 downregulation and an increased Th17-related immune response. The esophageal intraluminal environment, represented by the esophageal microbiota, could be associated with the development and exacerbation of achalasia.

Keywords: Th-17; myosin light chain phosphorylation; protein kinase C-potentiated phosphatase-inhibitor protein of 17 kDa

Introduction

Achalasia is an esophageal motility disorder characterized by the impaired relaxation of the lower esophageal sphincter (LES) during swallowing and the absence of peristalsis. Owing to dysphagia and the associated chest pain, achalasia negatively impacts the quality of life and increases the risk of developing aspiration pneumonia [1, 2]. Although high-resolution manometry (HRM) and the Chicago classification have improved the clinical diagnosis of achalasia [3, 4], its etiology and pathophysiology remain unknown. Achalasia is an immune-mediated inflammatory disease associated with human herpes simplex virus type 1 (HSV-1) [5-7]. Patients with achalasia present with not only HSV-1-associated Th1-related immune responses, but also with Th2- and Th17-related immune responses [6]. Therefore, the development of achalasia is not only limited to HSV-1 infection [8], but also to other unknown environmental and genetic factors. Furthermore, the association of the immune-inflammatory response with the altered contractile state of the esophageal smooth muscle, observed in patients with achalasia whose myenteric ganglion cells are still intact, is unclear.

The contractile state of smooth muscles is regulated by phosphorylation of the 20-kDa myosin regulatory light chain (LC_{20}), which is controlled by the balance between the opposing activities of myosin light chain kinase (MLCK) and myosin light chain phosphatase (MLCP) [9]. The protein kinase C-potentiated phosphatase inhibitor of 17 kDa (CPI-17) regulates MLCP activity [10]. LC_{20} phosphorylation is differentially regulated in gastrointestinal and vascular smooth muscles through MLCP activity [11]. A change in CPI-17 expression is associated with the dysregulation of LC_{20} phosphorylation and dysmotility of the smooth muscle tissues under pathological conditions, such as hypertension, inflammatory bowel disease, and erectile dysfunction [12]. However, the regulation of LC_{20} phosphorylation, its association with the contractile properties of LES, and its role in achalasia remains unknown. Cytokines, such as TNF-α and IL-1β [13], reduce gastrointestinal contractility by downregulating CPI-17 and increasing MLCP activity. Therefore, an alteration in LES LC_{20} phosphorylation status may contribute to the pathogenesis of achalasia.

Microbiome alterations play a role in the pathogenesis of inflammatory conditions in the gastrointestinal tract. Thus, changes in the esophageal microbiota may be associated with

the immune-inflammatory response, observed in patients with achalasia whose myenteric ganglion cells are still intact. Nonetheless, whether the esophageal microbiota is involved in the pathogenesis of achalasia remains to be determined.

Therefore, we aimed to determine the effect of LC_{20} phosphorylation status on LES and the role of the esophageal microbiota in the immune-inflammatory response observed in patients with achalasia.

Materials and Methods

Materials

Reagent-grade chemicals were used. Nicotine, carbachol (CCh), Substance P, and Pefabloc SC were purchased from Sigma-Aldrich (St. Louis, MO, USA). Trichloroacetic acid (TCA), dithiothreitol, and acetone were purchased from Fujifilm Wako Pure Chemicals (Osaka, Japan). Pan anti-LC_{20} (sc-15370) and mouse monoclonal anti-α-SMA (sc-53015) antibodies were purchased from Santa Cruz Biotechnology (Dallas, TX, USA). Anti-HuC/HuD neuronal protein, mouse IgG2, biotin-XX conjugate (A21272) Streptavidin, and Alexa Fluor™ 488 conjugate (S32354) were purchased from Thermo Fisher Scientific (Waltham, Massachusetts, USA)

Methods

Esophageal sample collection from patients with achalasia

Informed consent was obtained from 30 patients with type II achalasia who underwent peroral endoscopic myotomy (POEM) at Kyushu University Hospital or Showa University Koto Toyosu Hospital between October 2017 and March 2021. POEM is a standard, less invasive technique for achalasia than Heller myotomy [14] and allows easy procurement of biopsy samples from smooth muscle tissues at the disease site. The aim of the study was explained to each patient during a medical interview before POEM, endoscopic submucosal dissection (ESD), or surgery. All patients were informed of the potential risk of bleeding from the biopsy sites and perforation of the muscularis propria during POEM. Only patients who provided written informed consent were included. This study was reviewed and approved by

the Ethics Committees of Kyushu University (2020-774), Showa University Koto Toyosu Hospital (17T5001), and Okayama University of Science (3-4). The study adhered to the ethical principles of the Declaration of Helsinki. Type II achalasia was diagnosed based on the Chicago Classification ver3.0 [3]. Muscular samples of LES were obtained from 20 patients to measure LC_{20} phosphorylation and CPI-17 expression (Study 1). Mucosal samples of the esophageal body and muscle samples of LES were obtained from 16 patients to examine Th1-, Th2-, and Th17-related cytokine expression and determine the proteins associated with contractile function. Additionally, 16S rRNA amplicon sequencing was performed on these samples to analyze the esophageal microbiota. This was partially combined with *in situ* hybridization for esophageal microbiota (Study 2). Six patients provided samples for studies 1 and 2. Characteristics of the patients with achalasia enrolled in the studies (1 and 2) are summarized. In Study 3, we collected esophageal conditioned media from a 61-year-old female patient diagnosed with type II achalasia, who underwent POEM on August 15, 2022. Her HRM examination and cytokine profile analysis confirmed the typical features of type II achalasia, as detailed in Supplemental Table 1. As a control patient, we included a 73-year-old male who, despite being asymptomatic, had early gastric cancer who underwent ESD on August 15, 2022. Control mucosal samples of the esophageal body were obtained from 11 asymptomatic patients with early gastric cancer who underwent ESD, and control muscular samples of LES were obtained from 16 asymptomatic patients with esophageal cancer who underwent surgery. To determine LC_{20} phosphorylation and CPI-17 expression, the LES samples were soaked in normal extracellular solution (NES) (in mM: 37.4 NaCl, 5.9 KCl, 1.2 $CaCl_2$, 1.2 $MgCl_2$, 11.5 glucose, and 11.6 HEPES; pH 7.4) immediately after biopsy and prepared, as described in the subsequent section. For 16S sequencing and to determine mRNA expression, the mucosal and muscle samples were soaked in RNAlater (Thermo Fisher Scientific, MA, USA) immediately after biopsy and stored at −30 ℃ until further use.

Myosin light chain (LC_{20}) phosphorylation analysis

LES biopsy samples were soaked in NES immediately after the biopsy. During the equilibration period, the tissues were stimulated five times with 118 mM K^+ extracellular

solution (KES) every 2 min. KES (isotonic) was prepared by replacing NaCl with equimolar KCl in NES. KES composition was as follows (in mM): 25.3 NaCl, 118.0 KCl, 1.2 $CaCl_2$, 1.2 $MgCl_2$, 11.5 glucose, and 11.6 HEPES; pH 7.4. After the equilibration period, tissues were treated with 1 μM nicotine, 10 μM CCh, or 1 μM substance P for 1 min. The stimulated tissues were homogenized in cold TCA, 10 mM dithiothreitol, and 4 mM PefablocSC in acetone and frozen at −20 °C overnight. Phosphorylation levels of LC_{20} in LES were determined using phos-tag SDS-PAGE combined with western blotting, as previously described [15, 16]. The TCA/acetone-fixed tissues were washed twice with cold acetone and vacuum-dried. Proteins were extracted by immersing dried tissues in 1x lithium dodecyl sulfate (LDS) sample buffer [2% (w/v) LDS], 6 M urea, 2 M thiourea, 65 mM Tris-HCl (pH 6.8), 100 mM dithiothreitol, 10% glycerol, and 0.01% (w/v) bromophenol blue (BPB) and vigorously agitating for 1 h at 23 ℃. LC_{20} proteins were separated, based on their phosphorylated states, using phos-tag SDS-PAGE [17] and western blotting with pan anti-LC_{20} antibody. The stoichiometry of LC_{20} phosphorylation was calculated using the following equation:

$$\text{Moles of } P_i \text{ per mole of } LC_{20} = y / (x + y) \quad (1)$$

where x and y are the signal intensities of the unphosphorylated and monophosphorylated LC_{20} bands, respectively.

Western blot analysis for CPI-17 in LES

Proteins were extracted from the TCA/acetone-treated LES tissue, as described above, and loaded onto 7.2% Laemmli polyacrylamide gels. Electrophoresis was performed using AllView PAGE Buffer (BioDynamics Laboratory Inc., Tokyo, Japan). CPI-17 and α-smooth muscle actin (α-SMA) were quantified by western blot analysis [15] using rabbit polyclonal anti-CPI-17 antibodies [18] and mouse monoclonal anti-α-SMA antibodies, respectively. Horseradish peroxidase was detected using Clarity Western ECL Substrate (Bio-Rad Laboratories, Hercules, CA, USA) or ECL Select Reagent (GE Healthcare Life Sciences, Pittsburgh, PA, USA). The emitted light was detected and quantified using a CCD imager (Amersham680, GE Healthcare Life Sciences). Relative CPI-17 expression levels were normalized to those of α-SMA.

RNA extraction and quantitative real-time polymerase chain reaction (qPCR)

RNA extraction and qPCR were performed, as described previously [19]. Total RNA was purified from whole biopsy specimens using the TRIzol reagent (Thermo Fisher Scientific, Massachusetts, United States). Total RNA (2 μg) was reverse-transcribed using a QuantiTect Reverse Transcription kit (QIAGEN, Düsseldorf, Germany) to obtain cDNA. Targeted cytokine, transcription factor, and contraction-associated protein expression levels were examined by qPCR using FAM-labeled TaqMan Gene Expression Assay Reagent (Thermo Fisher Scientific, Massachusetts, United States). The qPCR reaction conditions were as follows: 95 ℃ for 10 min, 45 cycles of 95 ℃ for 15 s, and 60 ℃ for 60 s. All assays were performed in duplicate. The Ct values of the genes of interest were normalized to those of the housekeeping gene, glyceraldehyde-3-phosphate dehydrogenase (*GAPDH*). The primers for the target genes are shown in Supplemental Table 2.

16S rRNA amplicon sequencing

The esophageal microbiota was examined using RNA-based 16S rRNA analysis. RNA-based 16S rRNA analysis reflects the transcriptional activity of microbes; therefore, it allows for the detection of only viable microbes (not dead or dormant microbes) [20, 21 22]. Oral microbes incessantly flow into the esophagus during swallowing, and esophageal contents often accumulate in patients with achalasia; therefore, RNA-based 16S rRNA analysis was selected. Total RNA was extracted from the whole biopsy specimens using the TRIzol reagent. The V1–V2 region of 16S rRNA was amplified from cDNA using the universal primers Tru 27F and Tru 354R36 (Supplemental Table 3). Reverse transcription was performed using the Tru 354R primer and PrimeScript II 1st Strand cDNA Synthesis Kit (Takara Bio, Shiga, Japan), according to the manufacturer's instructions. Reaction conditions for reverse transcription were: 42 °C for 45 min and 70 °C for 15 min. PCR was performed using the Takara Ex Taq HS DNA polymerase (Takara Bio, Shiga, Japan). Reaction conditions for PCR were as follows: 94 ℃ for 3 min, 30 cycles of 94 ℃ for 30 s, 50 ℃ for 30 s, 72 ℃ for 30 s, and 72 ℃ for 10 min. A barcode sequence tag was added to each amplicon in the second round of PCR. The conditions

of the second round of PCR were as follows: 94 °C for 3 min; 10 cycles of 94 ℃ for 30 s, 60 ℃ for 30 s, 72 ℃ for 30 s, and 72 ℃ for 10 min. At each step, the PCR products were purified using a QIAquick PCR Purification Kit (QIAGEN, Düsseldorf, Germany), according to the manufacturer's instructions. The 16S rRNA amplicon sequencing of the PCR products was conducted by the Bioengineering Lab. Co., Ltd. The PCR products were quantified using a Qubit 3.0 Fluorometer and a dsDNA HS Assay Kit (Thermo Fisher Scientific), and the quality was confirmed using a Fragment Analyzer (Advanced Analytical Technologies, Ankeny, IA, USA) with a dsDNA 915 Reagent Kit (Agilent, Santa Clara, CA, USA). Paired-end sequencing (2 × 300 bp) was performed using the Illumina MiSeq platform (Illumina, San Diego, CA, USA) and the MiSeq Reagent Kit v3 (Illumina). Reads that began with a sequence that completely matched the primers were extracted using the fastx barcode splitter tool in the FASTX Toolkit (ver. 0.0.14). Next, the reads were trimmed and filtered using the sickle tool with a quality value of 20. The trimmed and paired-end reads with fewer than 150 bases were discarded. Analysis of the 16S microbiome data was performed using QIIME2 [22, 23]. The primer, noise, and chimera sequences were removed using the DADA2 method, and representative sequences were extracted. Taxonomy was assigned to ASVs (amplicon sequence variants) using the feature-classifier plugin with 97% similarity to the Greengenes reference sequence database (ver.13_8). A phylogenetic tree was constructed using the alignment and phylogeny plugins.

α-Diversity analysis

The α-diversity of the esophageal microbiota composition was calculated using the Chao1 and Shannon indices, with the ASV table rarefied to 50,260 sequences per sample with 10 random interactions using the QIIME2 diversity plugin. The Pielo evenness index was calculated using Shannon's index.

β-Diversity analysis

The pairwise-weighted UniFrac distance of the esophageal microbiota composition between samples was calculated based on the ASV table rarefied to 16,969 sequences per sample using

the QIIME2 diversity plugin. Differences in community components were statistically analyzed based on the weighted and unweighted UniFrac metric using the "Adonis" function with 999 permutations in the QIIME 2 pipeline.

In situ hybridization for esophageal microbiota detection

To detect all bacteria, we used fluorescence *in situ* hybridization (FISH) analysis with the EUB338 Alexa 488 probe (5′- GCT GCC TCC CGT AGG AGT -3′) (Chromosome Science Laboratory Inc., Japan), according to the manufacturer's instructions. The tissue sections were deparaffinized, rehydrated, and subjected to antigen retrieval using 0.02–0.5% pepsin/0.1 N HCl for 30 min at 95 ℃. Subsequently, the tissue sections were washed with phosphate-buffered saline (PBS) and dehydrated using an alcohol series. For hybridization, 10 μL of the EUB 388 probe (30 ng/μL) was applied to the sections and covered with coverslips. Subsequently, denaturation was performed at 90 °C for 10 min on a hotplate. The sections were then hybridized at 37 ℃ for 10 h in a wet chamber. Later, the slides were washed twice with saline-sodium citrate (SSC) for 5 min, and the coverslips were gently removed. The slides were then incubated twice in SSC/0.3% NP-40 at 37 ℃ for 20 min and then in SSC for 15 min at room temperature. Finally, the slides were counterstained with 4',6-diamidino-2-phenylindole and mounted using an antifade mounting medium.

Transfer of esophageal conditioned media obtained from patients with achalasia into the mouse esophagus

Esophageal conditioned media was prepared by rinsing the esophageal mucosa in 40 mL of normal saline solution during esophagogastroduodenoscopy (in asymptomatic patients with early gastric cancer [control] and patients with achalasia). The esophageal conditioned media was collected and stored at −80 ℃ until further use. Male C57BL/6J mice (Charles River Laboratories Inc., Kanagawa, Japan) between seven and nine weeks of age were maintained in specific-pathogen-free facilities at Kyushu University, wherein the following experiments were conducted with the approval of the Committee on Animal Research of Kyushu University (Approval number for animal experiments: A22-261-0). We transferred 100 μL of esophageal

conditioned media per dose into the mice esophagus by oral gavage using a flexible cannula thrice a week for four weeks. The mice had no access to drinking water for 30 min post-gavage. The mice were then sacrificed, and the distal esophagus was collected. RNA extraction and gene expression analyses were performed, as described previously. The primers used for the target genes are listed in Supplemental Table 4

Immunohistochemical detection and quantification of ganglion cells in the treated mouse esophagus

Paraffin-embedded mouse esophageal tissue sections (4-μm thick) were deparaffinized and rehydrated using xylene and graded ethanol solutions. Antigen retrieval was performed by boiling the sections in 10 mM sodium citrate buffer (pH 6.0) for 15 min. The sections were then blocked with 5% normal goat serum in PBS for 1 h at room temperature. The primary antibody, HuC/HuD monoclonal antibody (16A11), which was biotin-conjugated (Thermo Fisher Scientific), was diluted 1:200 in PBS containing 1% BSA and incubated with the sections overnight at 4 °C. The sections were then washed with PBS and incubated with Alexa Fluor 555-conjugated streptavidin (Thermo Fisher Scientific), diluted 1:1000 in PBS for 1 h at room temperature. The sections were mounted with the DAPI-containing mounting medium (Vector Laboratories) and cover slips were added.

The ganglion cells in the myenteric plexus of the mouse esophagus were identified by HuC/HuD and DAPI staining. The sections were observed under a fluorescence microscope and images were obtained (KEYENCE BZ-X710). The number of ganglion cells per section was calculated by counting all the HuC/HuD- and DAPI-positive cells in the whole section.

Statistical analysis

All statistical analyses were performed using the JMP Pro software (version 16.0.0; SAS Institute, Inc., NC, USA). Graphs were constructed using JMP Pro or Prism software (version 9; GraphPad, CA, USA). All numerical data are expressed as medians and interquartile ranges, unless stated otherwise. The boxes represent 25–75% quartiles, and the whiskers indicate the minimum and maximum values. The Mann–Whitney U test was used to compare non-normally

distributed data between two groups. Esophageal microbiota composition was first evaluated using a linear discriminant analysis effect size (LEfSe) assessment [38], and trend analysis was performed using a linear trend test. β-Diversity was estimated using the UniFrac metric to calculate the distances of the esophageal microbiota composition between the samples, visualized by principal coordinate analysis (PCoA), and statistically analyzed using permutational multivariate analysis of variance (PERMANOVA). Results with $p<0.05$ were considered as statistically significant. Finally, linear regression analysis was used to determine the relationship between the two variables.

Results

Impaired LC_{20} phosphorylation in patients with achalasia

We determined the level of LC_{20} phosphorylation in LES tissues from patients with achalasia and non-achalasia controls (Study 1) using Phos-tag SDS-PAGE. As shown in **Fig. 1a and 1b**, under unstimulated conditions (NES), the level of LC_{20} phosphorylation in the LES of control patients was 24.7% (11.2–40.8%, n=13). Stimulation with nicotine (a nicotinic acetylcholine receptor agonist), CCh (a muscarinic acetylcholine receptor agonist), or substance P (an activator of the esophageal intramuscular ICC [26]) had no effect on the levels of LC_{20} phosphorylation. The levels of LC_{20} phosphorylation upon stimulation with 1 μM nicotine (P-LC_{20}=34.2% with a range of 20.0–40.0%, n=4), 10 μM CCh (22.9%, 14.1–36.1%, n=9), or 1 μM substance P (30.3%, 26.8–33.0%, n=4) were not significantly different from those under the resting condition (24.7%, 11.2–40.8%, n=13) (**Fig. 1b**). Contrarily, the levels of LC_{20} phosphorylation detected in the LES of patients with achalasia were negligible under unstimulated and agonist-stimulated conditions **(Fig. 1a**). The levels of LC_{20} phosphorylation upon stimulation with 1 μM nicotine (3.4%, 2.3–6.8%, n=9), 10 μM CCh (4.9%, 2.1–9.4%, n=15), and 1 μM substance P (7.1%, 3.4–9.4%, n=4) were also not significantly different from those under the resting condition (2.3%, 0–6.9%, n=20) (**Fig. 1b**). Simultaneously, the protein expression level of CPI-17 in the LES of patients with achalasia (0.67, 0.35–0.93, n=20) was significantly lower than that of control patients (0.97, 0.62–1.30, n=8). Thus, CPI-17 downregulation, which causes MLCP activity upregulation, leads to LC_{20} hypo-

phosphorylation in the LES of patients with achalasia (**Fig. 1c, d**). Notably, CPI-17 downregulation was not associated with a decline in MLCK and/or protein phosphatase 1δ (PP1δ; the catalytic subunit of MLCP) expression, suggesting a change in proteostasis (**Fig. 1e**, left). MLCK and/or PP1δ expression levels were similar in patients with achalasia and control patients (Study 2).

Upregulation of Th17-related cytokines in patients with achalasia

Cytokine profiles of the esophageal mucosa and muscle from patients with achalasia and control patients were investigated by determining the mRNA expression of Th1-related cytokines (TNF-α, IFN-γ, IL-1β, IL-12A, IL-12B), Th2-related cytokines (IL-4, IL-5, IL-13, IL-33), and Th-17-related cytokines (IL-17A, IL-17F, IL-21, IL-22, IL-23A, IL-6) (Study 2). The mRNA expression levels of the corresponding transcription factors (TBX21, GATA3, and RORC) were also examined. In the mucosa tissues derived from patients with achalasia, IFN-γ was significantly upregulated. In addition, TNF-α and IL-12A levels were downregulated. No significant differences were observed in Th2-related cytokine levels between the two patient groups. GATA3 was downregulated in patients with achalasia. IL-17A, IL-17F, IL-22, and IL-23A levels were significantly higher in patients with achalasia than in control patients (**Fig. 2a**). In the smooth muscle tissues, IL-13 was downregulated. There were no significant differences in the expression of Th1, Th2, and Th17-related cytokines, except for IL-6, between the patient groups (**Fig. 2b**). Overall, Th17-related cytokines were upregulated in the esophageal mucosa and showed downregulation of LC_{20} phosphorylation signaling in the LES smooth muscles of patients with achalasia.

Esophageal microbiota composition was altered in patients with achalasia

To test whether the esophageal microbiota is involved in cytokine release from the mucosa, we compared the esophageal microbiota composition between patients with achalasia (n=16) and control patients (n=11) using RNA-based 16S rRNA analysis (Study 2). The Chao1 (species richness) and Shannon (species diversity) indices of the mucosa were significantly higher in patients with achalasia than in control patients ($p<0.05$) (**Fig. 3a**). Furthermore, there

was a significant difference in the esophageal microbiota composition, determined by weighted UniFrac distances (PERMANOVA, p=0.014), between the two patient groups (**Fig. 3b**, right). At the phylum level, the proportions of *Bacteroides* and *Actinobacteria* were significantly higher in patients with achalasia than in control patients. At the genus level, the findings showed that the proportions of *Streptococcus*, *Helicobacter pylori*, and *Xanthomonas* were significantly lower in patients with achalasia, whereas those of several microbes, including *Actinomyces* and *Dialister*, were significantly higher than in control patients. *In situ* hybridization confirmed the presence of microbes in the esophageal mucosa of patients with achalasia (**Fig. 3d**, arrows).

Esophageal microbes associated with Th17-related cytokines expression

We determined the association (at the genus level) between esophageal microbes and esophageal mucosal Th17 immune responses (Study 2) (**Fig. 4**). Among the compositions that were significantly different between the two patient groups, the proportion of *Actinomyces* significantly positively correlated with IL-23A (r=0.53, p=0.005) (**Fig. 4**, top). The population of *Dialister* was significantly positively associated with IL-17A (r=0.46, p=0.02), IL-17F (r=0.49, p=0.01), and IL-22 (r=0.48, p=0.01) (**Fig. 4**, bottom), linking at least two groups of microbes to the pathologic response in the mucosa.

Elevated cytokine expression and histological findings in the esophagus of mice treated with esophageal conditioned medium obtained from patients with achalasia

To determine whether the esophageal intraluminal environment, including microbes, induces a Th17-related immune response, we collected esophageal conditioned media from patients with achalasia and transferred them to the SPF-mouse esophagus by oral gavage (Study 3). Following a four-week treatment with conditioned media or saline as a control, cytokine expression was determined using qPCR (Fig 5). Both IL-17F (p=0.01, n=5) and IL-1β (p=0.007, n=5) were significantly elevated, and IL-23A (p=0.060, n=5) tended to be upregulated in the mouse esophagus treated with esophageal conditioned media from patients with achalasia compared with that in mice treated with the saline control. Contrarily, no significant difference was observed in cytokine expression in the esophagus treated with saline and that treated with

esophageal conditioned media from patients with early gastric cancer. Consistent with the cytokine profiles, ganglion cells decreased in the mouse esophagus treated with esophageal conditioned media from patients with achalasia (n=4) when compared with that in mice treated with saline control (n=4), 107±12.6 vs 59±18.1, p=0.01. Esophageal conditioned media with the microbiota of patients with achalasia could mimic the inflammatory response of the mucosa linked to LES smooth muscle dysmotility.

Discussion

To the best of our knowledge, our study is the first to demonstrate that LC_{20} phosphorylation in the LES is significantly impaired and that esophageal microbiota is highly associated with the Th17-related immune response observed in these patients. We further showed that the esophageal environment is a potential factor in the pathophysiology of achalasia. We also found that a considerable amount of LC_{20} phosphorylation occurred even under unstimulated conditions in the LES of control patients. Contrarily, negligible LC_{20} phosphorylation has been observed under unstimulated conditions in the renal vasculature [27] and intestinal non-sphincter smooth muscles [11]. In the human LES, high levels of LC_{20} phosphorylation remain unchanged by agonist stimuli, such as nicotine, substance P, and CCh, which stimulate ganglionic nicotinic acetylcholine receptors located in Auerbach's plexus, neurokinin 1 receptors located in the ICC [26], and muscarinic acetylcholine receptors located in smooth muscle, respectively. Notably, the level of LC_{20} phosphorylation did not correlate with the extent of LES contractility. These results indicate the differential roles of LC_{20} phosphorylation in smooth muscle contractility between non-sphincter and sphincter smooth muscles. Further investigation in human tissues is necessary to elucidate the effect of LC_{20} phosphorylation in the LES, which spontaneously contracts by default and relaxes upon stimulation.

Based on an HRM study showing that both relaxant and contractile responses of the LES are impaired in patients with achalasia, we postulated that a certain level of basal LC_{20} phosphorylation is necessary for maintaining an appropriate LES contractile state that can relax or contract depending on the type of stimulus. LC_{20} phosphorylation is controlled by the balance

between the opposing activities of MLCK and MLCP [9]. MLCK activity is dependent on Ca^{2+}-calmodulin, whereas MLCP activity is regulated either directly by phosphorylation of the myosin-targeting subunit of MLCP (MYPT-1) [28] or indirectly via CPI-17 [10]. Therefore, a decrease in CPI-17 activity leads to a reduction in LES phosphorylation through an increase in MLCP activity. There was no difference in the expression of MLCK or PP1δ between the two patient groups. Therefore, CPI-17 downregulation likely accounted for MLCP hyper-activation and LC_{20} hypo-phosphorylation in patients with achalasia. Our study suggests that decreased CPI-17 levels can be attributed to CPI-17 degradation as the CPI-17 mRNA was upregulated, possibly by a feedback mechanism. CPI-17 is downregulated during intestinal inflammation and alters smooth muscle contractility in animal models [13] and patients with ulcerative colitis [29]. CPI-17 may be downregulated in patients with achalasia in a manner similar to that observed in patients with ulcerative colitis. Th-2 and Th-17-related immune responses are involved in ulcerative colitis. Therefore, the Th17-related immune response elicited by patients with achalasia may downregulate CPI-17; however, TNF-α and IL-1β induced CPI-17 downregulation in an animal model, which is likely mediated through translational regulation [30]. To establish the pathways through which Th-17-related cytokines downregulate CPI-17 as potential targets for achalasia treatment, the underlying mechanisms must be fully elucidated.

The type of Th immune responses involved in patients with achalasia is undetermined. A previous study reported that every Th-1, Th-2, and Th-17-related immune response is upregulated in type II achalasia [6]. Contrarily, we found that only Th-17-related immune responses, including IL-17A, IL-17F, IL-22, and IL-23A, were upregulated in type II achalasia mucosa. We anticipate that the discrepancy in cytokine profiles between the previous and present studies is due to the difference in quantification methods: immunohistochemistry [6] vs. qPCR in this study. Further studies are required to understand the cytokine profiles associated with achalasia. However, it can be concluded that the Th17-related immune response is involved in achalasia pathogenesis. In this study, no cytokines were upregulated in the muscularis propria of patients with achalasia. Considering that the control samples of the muscularis propria were obtained from patients with esophageal cancer, IL-6 expression in control subjects was likely to be upregulated [31-34]. Moreover, IL-13 was downregulated in

the muscle layer. As a key cytokine in the Th2 immune response, this downregulation may promote upregulation of the Th17 immune response, which is implicated in the pathogenesis of achalasia.

Gut microbiota is highly associated with the induction of Th17 cells [35, 36]. Therefore, the esophageal environment represented by the esophageal microbiota may influence the upregulation of the Th-17-related immune response in patients with achalasia. The esophageal mucosa hosts the resident microbiota, although the esophageal microbiota population (10 per g/mL of sampled material) is much smaller than that of the large intestine (10^{12} per g/mL of sampled material) [37]. The number of studies on esophageal microbiota remains limited due to difficulties in obtaining esophageal samples. The prevalence of *Streptococcus*, *Fusobacterium*, *Veillonella*, and *Prevotella* in healthy individuals has been reported in several studies [37-41]. Among these, *Streptococcus* was detected in high proportions in healthy subjects in all the studies, indicating that *Streptococcus* may play a role in maintaining the esophageal environment. Several studies have suggested possible links between esophageal microbiota and esophageal diseases, such as gastroesophageal reflux disease [42, 43], eosinophilic esophagitis [44, 45], and esophageal squamous cell cancer [46, 47]. Here, we proposed that the esophageal microbiota is altered, with an increase in α-diversity and changes in β-diversity. The proportion of *Streptococcus* was altered the most in patients with achalasia. Furthermore, both *Actinomyces and Dialister* are associated with increased Th17-related immune responses in patients with achalasia. Importantly, the transfer of esophageal conditioned media from patients with achalasia to the mice esophagus increased Th17-related cytokines and decreased ganglion cells, mimicking achalasia pathogenesis. The esophageal intraluminal environment, represented by dysbiosis of the esophageal microbiota, contributes to the development and/or exacerbation of achalasia. In this study, microbiota diversity was high in the tissues of patients with achalasia. In contrast, decreased diversity was reportedly associated with intestinal diseases, such as inflammatory bowel disease [20,48-49]. It remains unclear how increased esophageal diversity leads to pathological conditions. Further studies are required to confirm the underlying pathogenic mechanisms.

This study had some limitations. First, the subjects of this study were all type II achalasia, which is the most common subtype [50, 51]. Previous studies have shown that the immune response in the esophagus was different among subtypes [52]; thus, there is a possibility that the other subtypes could show different cytokine profiles. Comparing the subtypes of achalasia is essential for a comprehensive understanding of its pathogenesis. However, this is beyond the scope of our present study. We intend to pursue this question in our future work. Second, HRM was not conducted in the control group due to ethical considerations. Therefore, there is a low possibility that the control subjects may have been in the early stages of achalasia, although the control subjects were asymptomatic. Third, control muscular samples were obtained from patients with esophageal cancer who underwent surgery. These samples may have been affected by the condition of esophageal cancer and/or by prior neoadjuvant chemotherapy or radiation therapy (used in esophageal cancer treatment). Finally, the transfer of esophageal conditioned media from patients with achalasia to the esophagus of mice increased the Th17-related cytokine levels; however, it is unclear whether this caused the development of achalasia-like esophageal dysmotility. Additionally, although the mucosal layer is similar between mice and humans, the muscular layer of the mouse esophagus differs from that of humans. The mouse esophagus is composed mostly of striated muscle, while the human esophagus is composed of striated muscle in the oral one-third and smooth muscle in the anal two-thirds. Validating the pathogenesis of achalasia at the smooth muscle level is technically difficult. Achalasia is a human-specific disease; therefore, the present study focused on using human samples. Nonetheless, it is noteworthy that the transfer of conditional media from patients with achalasia to the mouse esophagus mimics the immune response characterized in this study.

In conclusion, increased Th17-related immune response and impairment of LC_{20} phosphorylation in the LES with CPI-17 downregulation were associated with achalasia. The esophageal microbiota is associated with the development and/or exacerbation of achalasia. The esophageal microbiota, Th-17-related immune response, and CPI-17 and LC_{20} phosphorylation status may contribute to the development of novel treatments for achalasia.

Grant Support:

This study was supported in part by the Japan Society for the Promotion of Science KAKENHI (20K08334, 22K19530, 23K07440) and the Japan Agency for Medical Research and Development (AMED) (21lk0201144h001, 22lk0201144h002, and 23lk0201144h003).

Disclosure:

The authors declare no conflicts of interest related to this study.

References

1. Boeckxstaens GE, Zaninotto G, Richter JE. Achalasia. Lancet. 2014;383:83–93.
2. Islam S. Achalasia. Semin Pediatr Surg. 2017;26:116–20.
3. Kahrilas PJ, Bredenoord AJ, Fox M, et al. The Chicago Classification of esophageal motility disorders, v3.0. Neurogastroenterol Motil. 2015;27:160–74.
4. Yadlapati R, Kahrilas PJ, Fox MR, et al. Esophageal motility disorders on high-resolution manometry: Chicago classification version 4.0©. Neurogastroenterol Motil. 2021;33:e14058.
5. Clark SB, Rice TW, Tubbs RR, et al. The nature of the myenteric infiltrate in achalasia: An immunohistochemical analysis. Am J Surg Pathol. 2000;24:1153–8.
6. Furuzawa-Carballeda J, Aguilar-León D, Gamboa-Domínguez A, et al. Achalasia--an autoimmune inflammatory disease: A cross-sectional study. J Immunol Res. 2015;2015:729217.
7. Kahrilas PJ, Boeckxstaens G. The spectrum of achalasia: lessons from studies of pathophysiology and high-resolution manometry. Gastroenterology. 2013;145:954–65.
8. Boeckxstaens GE. Achalasia: virus-induced euthanasia of neurons? Am J Gastroenterol. 2008;103:1610–2.
9. Somlyo AP, Somlyo AV. Ca^{2+} sensitivity of smooth muscle and nonmuscle myosin II: modulated by G proteins, kinases, and myosin phosphatase. Physiol Rev. 2003;83:1325–58.

10. Eto M, Senba S, Morita F, et al. Molecular cloning of a novel phosphorylation-dependent inhibitory protein of protein phosphatase-1 (CPI17) in smooth muscle: its specific localization in smooth muscle. FEBS Lett. 1997;410:356–60.
11. Ihara E, Moffat L, Ostrander J, et al. Characterization of protein kinase pathways responsible for Ca^{2+} sensitization in rat ileal longitudinal smooth muscle. Am J Physiol Gastrointest Liver Physiol. 2007;293:G699–710.
12. Eto M, Kitazawa T. Diversity and plasticity in signaling pathways that regulate smooth muscle responsiveness: Paradigms and paradoxes for the myosin phosphatase, the master regulator of smooth muscle contraction. J Smooth Muscle Res. 2017;53:1–19.
13. Ohama T, Hori M, Momotani E, et al. Intestinal inflammation downregulates smooth muscle CPI-17 through induction of TNF-alpha and causes motility disorders. Am J Physiol Gastrointest Liver Physiol. 2007;292:G1429–38.
14. Inoue H, Sato H, Ikeda H, et al. Per-oral endoscopic myotomy: A series of 500 patients. J Am Coll Surg. 2015;221:256–264.
15. Takeya K, Kaneko T, Miyazu M, et al. Addition of urea and thiourea to electrophoresis sample buffer improves efficiency of protein extraction from TCA/acetone-treated smooth muscle tissues for phos-tag SDS-PAGE. Electrophoresis. 2018;39:326–333.
16. Takeya K, Loutzenhiser K, Shiraishi M,et al. A highly sensitive technique to measure myosin regulatory light chain phosphorylation: the first quantification in renal arterioles. Am J Physiol Ren Physiol. 2008;294:F1487–92.
17. Kinoshita E, Kinoshita-Kikuta E, Takiyama K, et al. Phosphate-binding tag, a new tool to visualize phosphorylated proteins. Mol Cell Proteomics. 2006;5:749–757.
18. Woodsome TP, Eto M, Everett A, et al. Expression of CPI-17 and myosin phosphatase correlates with Ca(2+) sensitivity of protein kinase C-induced contraction in rabbit smooth muscle. J Physiol. 2001;535:553–564.

19. Iboshi Y, Nakamura K, Fukaura K, et al. Increased IL-17A/IL-17F expression ratio represents the key mucosal T helper/regulatory cell-related gene signature paralleling disease activity in ulcerative colitis. J Gastroenterol. 2017;52:315–326.
20. Nishihara Y, Ogino H, Tanaka M, et al. Mucosa-associated gut microbiota reflects clinical course of ulcerative colitis. Sci Rep. 2021;11:13743.
21. De Vrieze J, Pinto AJ, Sloan WT, et al. The active microbial community more accurately reflects the anaerobic digestion process: 16S rRNA (gene) sequencing as a predictive tool. Microbiome. 2018;6:63.
22. Moen AEF, Lindstrøm JC, Tannæs TM, et al. The prevalence and transcriptional activity of the mucosal microbiota of ulcerative colitis patients. Sci Rep. 2018;8:17278.
23. Bolyen E, Rideout JR, Dillon MR, et al. Reproducible, interactive, scalable and extensible microbiome data science using QIIME 2. Nat Biotechnol. 2019;37:852–857.
24. Callahan BJ, McMurdie PJ, Rosen MJ, et al. DADA2: High-resolution sample inference from Illumina amplicon data. Nat Methods. 2016;13:581–583.
25. Segata N, Izard J, Waldron L, et al. Metagenomic biomarker discovery and explanation. Genome Biol. 2011;12:R60.
26. Xiaopeng B, Tanaka Y, Ihara E, et al. Trypsin induces biphasic muscle contraction and relaxation via transient receptor potential vanilloid 1 and neurokinin receptors 1/2 in porcine esophageal body. Eur J Pharmacol. 2017;797:65–74.
27. Takeya K, Wang X, Kathol I, et al. Endothelin-1, but not angiotensin II, induces afferent arteriolar myosin diphosphorylation as a potential contributor to prolonged vasoconstriction. Kidney Int. 2015;87:370–81.
28. Trinkle-Mulcahy L, Ichikawa K, Hartshorne DJ, et al. Thiophosphorylation of the 130-kDa subunit is associated with a decreased activity of myosin light chain phosphatase in alpha-toxin-permeabilized smooth muscle. J Biol Chem. 1995;270:18191–4.

29. Ohama T, Hori M, Fujisawa M, et al. Downregulation of CPI-17 contributes to dysfunctional motility in chronic intestinal inflammation model mice and ulcerative colitis patients. J Gastroenterol. 2008;43:858–65.
30. Kim JI, Urban M, Young GD, et al. Reciprocal regulation controlling the expression of CPI-17, a specific inhibitor protein for the myosin light chain phosphatase in vascular smooth muscle cells. Am J Physiol Cell Physiol. 2012;303:C58–68.
31. Fujiwara H, Suchi K, Okamura S, et al. Elevated serum CRP levels after induction chemoradiotherapy reflect poor treatment response in association with IL-6 in serum and local tumor site in patients with advanced esophageal cancer. J Surg Oncol. 2011;103:62–68.
32. Qiu JG, Wang L, Liu WJ, et al. Apigenin inhibits IL-6 transcription and suppresses esophageal carcinogenesis. Front Pharmacol. 2019;10:1002.
33. Soares-Lima SC, Gonzaga IM, Camuzi D, et al. IL6 and BCL3 expression are potential biomarkers in esophageal squamous cell carcinoma. Front Oncol. 2021;11:722417.
34. Wang LS, Chow KC, Wu CW. Expression and up-regulation of interleukin-6 in oesophageal carcinoma cells by n-sodium butyrate. Br J Cancer. 1999;80:1617–1622.
35. Atarashi K, Tanoue T, Ando M, et al. Th17 cell induction by adhesion of microbes to intestinal epithelial cells. Cell 2015;163:367–80.
36. Honda K, Littman DR. The microbiota in adaptive immune homeostasis and disease. Nature. 2016;535:75–84.
37. Di Pilato V, Freschi G, Ringressi MN, et al. The esophageal microbiota in health and disease. Ann N Y Acad Sci. 2016;1381:21–33.
38. Fillon SA, Harris JK, Wagner BD, et al. Novel device to sample the esophageal microbiome--the esophageal string test. PLoS One. 2012;7:e42938.
39. Gagliardi D, Makihara S, Corsi PR, et al. Microbial flora of the normal esophagus. Dis Esophagus. 1998;11:248–250.
40. Norder Grusell E, Dahlén G, Ruth M, et al. Bacterial flora of the human oral cavity, and the upper and lower esophagus. Dis Esophagus. 2013;26:84–90.

41. Pei Z, Bini EJ, Yang L, et al. Bacterial biota in the human distal esophagus. Proc Natl Acad Sci U S A. 2004;101:4250–5.
42. Liu N, Ando T, Ishiguro K, et al. Characterization of bacterial biota in the distal esophagus of Japanese patients with reflux esophagitis and Barrett's esophagus. BMC Infect Dis. 2013;13:130.
43. Yang L, Lu X, Nossa CW,et al. Inflammation and intestinal metaplasia of the distal esophagus are associated with alterations in the microbiome. Gastroenterology. 2009;137:588–597.
44. Benitez AJ, Hoffmann C, Muir AB, et al. Inflammation-associated microbiota in pediatric eosinophilic esophagitis. Microbiome. 2015;3:23.
45. Harris JK, Fang R, Wagner BD, et al. Esophageal microbiome in eosinophilic esophagitis. PLoS One. 2015;10:e0128346.
46. Yang L, Chaudhary N, Baghdadi J, et al. Microbiome in reflux disorders and esophageal adenocarcinoma. Cancer J. 2014;20:207–210.
47. Yang L, Francois F, Pei Z. Molecular pathways: pathogenesis and clinical implications of microbiome alteration in esophagitis and barrett esophagus. Clin Cancer Res 2012;18:2138–2144.
48. Ng SC, Bernstein CN, Vatn MH, et al. Geographical variability and environmental risk factors in inflammatory bowel disease. Gut. 2013;62:630–649.
49. Zuo T, Lu XJ, Zhang Y, et al. Gut mucosal virome alterations in ulcerative colitis. Gut. 2019;68:1169–1179.
50. Japan Esophageal Society. Descriptive rules for achalasia of the esophagus, June 2012: 4th Edition. Esophagus 2017;14:275–289.
51. Jankovic J, Milenkovic B, Skrobic O, et al. Achalasia subtype differences based on respiratory symptoms and radiographic findings. Diagnostics (Basel) 2023;13:2198.
52. Crespin OM, Tatum RP, Xiao K, et al. The relationship between manometric subtype and outcomes of surgical treatment for patients with achalasia: Achalasia: manometric subtypes. Surg Endosc 2017;31:5066–5075.

53. Patel DA, Lappas BM, Vaezi MF. Diagnostics (Basel). An overview of achalasia and its subtypes. Gastroenterol Hepatol (N Y) 2017;13:411–421.

Fig. 1 Alteration of contraction-associated proteins in patients with achalasia

a, b: Representative blots (**a**) and cumulative results (**b**) of myosin light chain (LC_{20}) phosphorylation levels in the lower esophageal sphincter (LES) smooth muscle tissues from control and achalasia groups analyzed using Phos-tag SDS-PAGE (Study 1). LES samples were soaked in 137-NES immediately after biopsy and treated with 1 μM nicotine, 10 μM CCh, and 1 μM substance P for 1 min. The stimulated tissues were frozen quickly in cold 10% TCA, 10 mM dithiothreitol, and 4 mM PefablocSC in acetone. 0P-LC_{20} and 1P-LC_{20} indicate non-phosphorylated and monophosphorylated LC_{20}, respectively. The stoichiometry of LC_{20} phosphorylation was calculated using the following equation: moles of Pi per mole of LC_{20} = y / (x + y), where x and y are the signal intensities of the unphosphorylated and monophosphorylated LC_{20} bands, respectively.

c, d: Representative blots (**c**) and cumulative results (**d**) of CPI-17 protein levels in LES smooth muscle tissues from the control group and patients with achalasia group analyzed using western blotting (Study 1). Relative CPI-17 protein expression levels were normalized to α-SMA.

e: Cumulative results of CPI-17, MLCK, and PP1δ expression in LES smooth muscle tissues from control and achalasia groups are shown (Study 2). The mRNA expression levels of these genes were shown as ΔCt values relative to those of glyceraldehyde-3-phosphate dehydrogenase (GAPDH). Each dot represents a single sample obtained from a single participant. The data are expressed as the median and interquartile range (a), the boxes represent 25–75%, and the whiskers indicate the minimum and maximum values (**c** and **d**). The Mann–Whitney U test was used to assess the differences between groups. *$p<0.05$, significantly different from the control; n.s., not significant.

Fig. 2 Cytokine profiles in the esophageal mucosa and muscle of Achalasia

a, b: Relative mRNA expression levels of the indicated cytokines in control (blue box) and achalasia (red box) in the mucosa (**a**) and smooth muscle (**b**) are shown (Study 2). Each dot

represents a single sample obtained from a single participant. The Ct values of the indicated cytokines were normalized to those of glyceraldehyde-3-phosphate dehydrogenase (*GAPDH*). The boxes represent 25–75%, and the whiskers indicate the minimum and maximum values. The Mann–Whitney U test was used to assess the differences between groups. * $p<0.05$, ** $p<0.01$, significant from the control; ns, not significant. TNF, tumor necrosis factor; IFN, interferon; IL, interleukin; TXB21, T-box transcription factor 21; GATA3, GATA-binding protein 3; RORC, RAR-related orphan receptor C.

Fig. 3 Alteration of esophageal microbiota in patients with achalasia

a, b: Comparison of esophageal microbiota composition between controls (blue box) and achalasia (red box) by α-diversity based on Chao1 and Shannon indices (**a**) and β-diversity based on unweighted and weighted UniFrac analysis (**b**) (Study 2). The boxes represent 25–75%, and the whiskers indicate the minimum and maximum values. The Mann–Whitney U test was used to assess the differences between groups. * $p<0.05$, significant compared with the control.

c: Differences in esophageal microbiota composition between control (blue) and achalasia (red) groups assessed using linear discriminant analysis (LDA) and linear discriminant analysis effect size (LEfSe) based on operational taxonomic units (Study 2).

d: Representative fluorescence image of the microbiota in the esophageal mucosa by *in situ* hybridization (yellow arrows) (Study 2).

Fig. 4 Esophageal microbiota associated with expression of Th17-related cytokines

Correlations between the mRNA expression of Th17-related cytokines and proportions of esophageal microbiota, including *Actinomyces* and *Dialister*, are shown (Study 2). The shadow represents the 95% confidence interval of the regression line.

Fig. 5 Cytokine expression in the esophagus of mice treated with esophageal conditioned medium (obtained from patients with achalasia)

a: Cumulative results of the relative cytokine expression in the esophagus of mice treated with normal saline solution or esophageal conditioned media obtained from asymptomatic patients with early gastric cancer (control) and achalasia are shown (Study 3). Cytokine expression is represented as ΔCt values relative to glyceraldehyde-3-phosphate dehydrogenase (GAPDH). Each dot represents a single sample obtained from a single participant. Analysis of variance (ANOVA) was performed to assess differences among the three groups. *$p<0.05$ and **$p<0.01$, significance between indicated groups; n.s., not significant. TNF, tumor necrosis factor; IFN, interferon; IL, interleukin.

b: Immunochemistry for HuC/D in the esophageal muscular layer of saline-transferred mouse HuC/HuD-positive cells.

c: Results are expressed as mean (lines) and dots (individuals) of HuC/HuD-positive cells in a whole section.

Table 1 Clinical characteristics of patients with achalasia enrolled in this study

	Study 1	Study 2
Number of patients	20	16
Age (year, median, and IQR)	60.5 (54.5–71.5)	65.5 (49.5–69.8)
Sex (number, M/F)	5/15	9/7
Eckard score	6.5 (5–9)	6 (3.8–9)
Disease duration (year, median, and IQR)	2 (1–3.75)	2 (1–9)
HRM parameters (ManoScan)		
Number of examinee with ManoScan	20	15
IRP (mmHg,)	31.7 (21.2–41.3)	24.3 (16.8–32.9)
Basal LES (mmHg)	45.5 (32.0–54.1)	38.4 (20.0–43.4)
HRM parameters (Starlet)		
Number of examinee with Starlet	0	1
IRP (mmHg)	-	24. 0
Basal LES (mmHg)	-	36.0
Morphologic type		
Straight type	15	12
Sigmoid type	4	3
Advanced sigmoid type	1	1
Dilatation grading		
Grade I (d < 3.5 cm)	10	7
Grade II (3.5 ≤ d < 6.0 cm)	9	9
Grade III (6.0 cm ≤ d)	1	0

IRP: integrated relaxation pressure. Morphologic type and dilatation grading were determined based on Descriptive Rules for Achalasia of the Esophagus, June 2012: 4th Edition [50].

Journal of Gastroenterology

Supplementary Materials for

Exploring the Link between Esophageal Microbiota Disturbances and Achalasia Development

Hiroko Ikeda[1], Eikichi Ihara[1]*, Kosuke Takeya[2], Koji Mukai[1], Manabu Onimaru[3], Kenoki Ouchida[4], Yoshitaka Hata[1], Xiaopeng Bai[1], Yoshimasa Tanaka[1], Taisuke Sasaki[5], Fumio Saito[2], Masumi Eto[2], Jiro Nakayama[6], Yoshinao Oda[5], Masafumi Nakamura[4], Haruhiro Inoue[3], and Yoshihiro Ogawa[1]

Correspondence to:

Eikichi Ihara M.D., Ph.D.

Department of Medicine and Bioregulatory Science, Graduate School of Medical Sciences, Kyushu University

3-1-1 Maidashi, Higashi-ku, Fukuoka-shi, Fukuoka 812-8582, Japan

E-mail: ihara.eikichi.167@m.kyushu-u.ac.jp

Telephone: +81-92-642-5286 Fax +81-92-642-5287

This file includes Supplementary Table S1 to S3

Supplementary Table 1. List of Genes Analyzed by Quantitative PCR for human		
Gene Symbol	Name	TaqMan Assay ID
TNF	Tumor necrosis factor	Hs00174128_m1
IFNG	Interferon gamma	Hs00989291_m1
IL12A	Interleukin 12A	Hs00168405_m1
IL12B	Interleukin 12B	Hs01011518_m1
IL1B	Interleukin 1beta	Hs01555410_m1
IL4	Interleukin 4	Hs00174122_m1
IL5	Interleukin 5	Hs01548712_g1
IL13	Interleukin 13	Hs00174379_m1
IL13	Interleukin 33	Hs01125943_m1
IL17A	Interleukin 17A	Hs00174383_m1
IL17F	Interleukin 17F	Hs00369400_m1
IL21	Interleukin 21	Hs00222327_m1
IL22	Interleukin 22	Hs01574154_m1
IL23A	Interleukin 23 subunit alpha	Hs00413259_m1
IL6	Interleukin 6	Hs00174131_m1
TBX21	T-box transcription factor 21	Hs00203436_m1
GATA3	GATA binding protein 3	Hs00231122_m1
RORC	RAR related orphan receptor C	Hs00172860_m1
PPP1R12	protein phosphatase 1 regulatory subunit 12A	Hs01552899_m1
PPP1R14	protein phosphatase 1 regulatory inhibitor subunit 14A	Hs00264434_m1
MYLK	Hs00364926_m1	Hs00364926_m1
GAPDH	Glyceraldehyde-3-phosphate dehydrogenase	Hs03929097_g1

Supplementary Table 2. Base sequence of the amplication primer(V1-V2 region of the 16S rRNA)	
	base sequence
Tru 27F	5'- CGCTCTTCCGATCTCTGAGRGTTTGATYMTGGCTCAG -3'
Try 354R	5'- TGCTCTTCCGATCTGACCTGCCTCCCGTAGGAGT -3'

Supplementary Table 3. List of Genes Analyzed by Quantitative PCR for mice		
Gene Symbol	Name	TaqMan Assay ID
TNF	Tumor necrosis factor	Mm00443258_m1
IFNG	Interferon gamma	Mm00801778_m1
IL1B	Interleukin 1beta	Mm00434228_m1
IL4	Interleukin 4	Mm00445259_m1
IL13	Interleukin 13	Mm00434204_m1
IL17A	Interleukin 17A	Mm00439619_m1
IL17F	Interleukin 17F	Mm00521423_m1
IL22	Interleukin 22	Mm00444241_m1
IL23A	Interleukin 23 subunit alpha	Mm00518984_m1
IL6	Interleukin 6	Mm00446190_m1
GAPDH	Glyceraldehyde-3-phosphate dehydrogenase	Mm99999915_g1

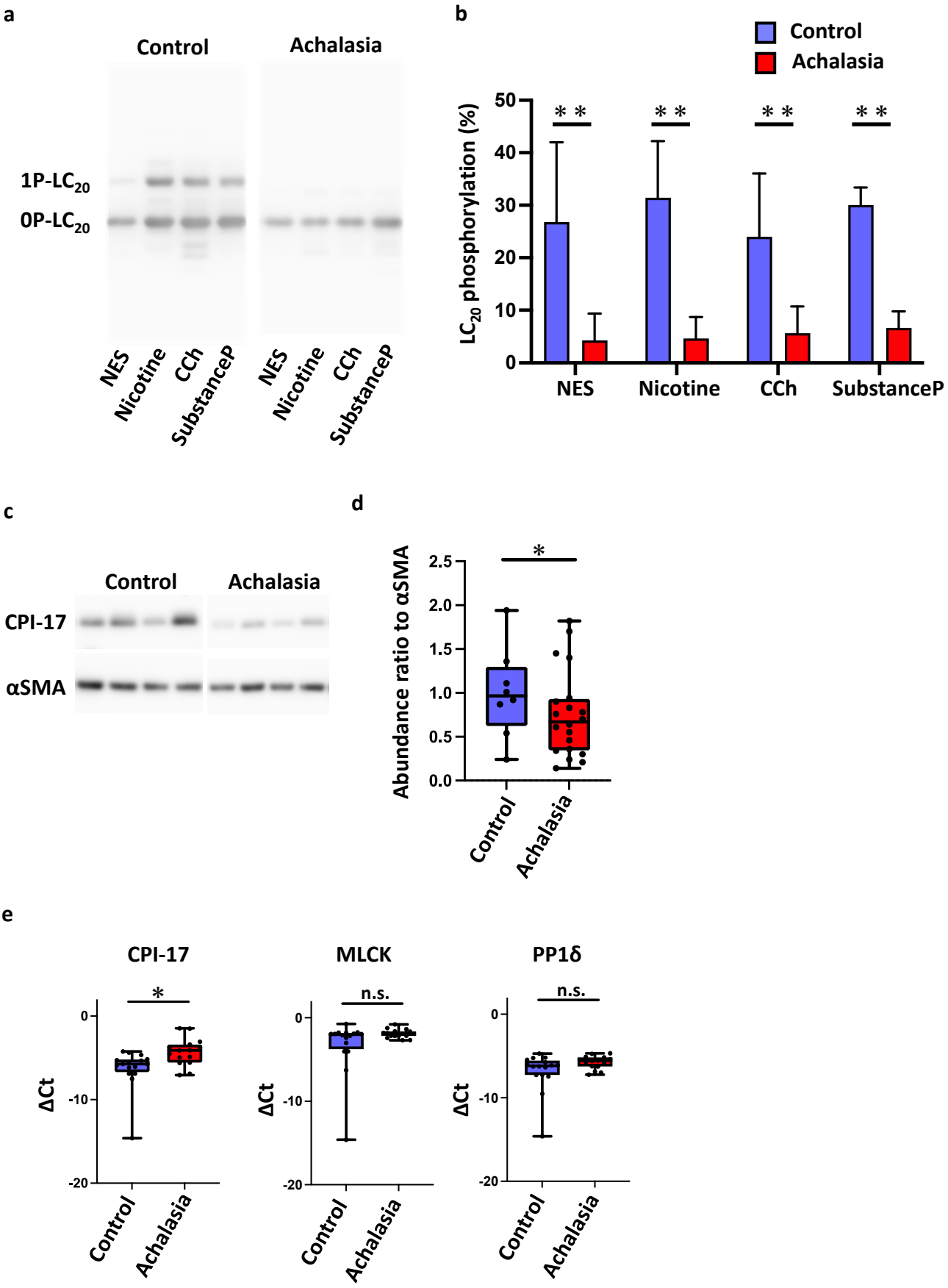
a
Control
Achalasia
1P-LC20
0P-LC20
NES
Nicotine
CCh
SubstanceP
b
Control
Achalasia
LC20 phosphorylation (%)
50
40
30
20
10
0
* *
NES
Nicotine
CCh
SubstanceP
c
Control
Achalasia
CPI-17
αSMA
d
Abundance ratio to αSMA
2.5
2.0
1.5
1.0
0.5
0.0
*
Control
Achalasia
e
CPI-17
MLCK
PP1δ
ΔCt
0
-10
-20
*
n.s.
Control
Achalasia

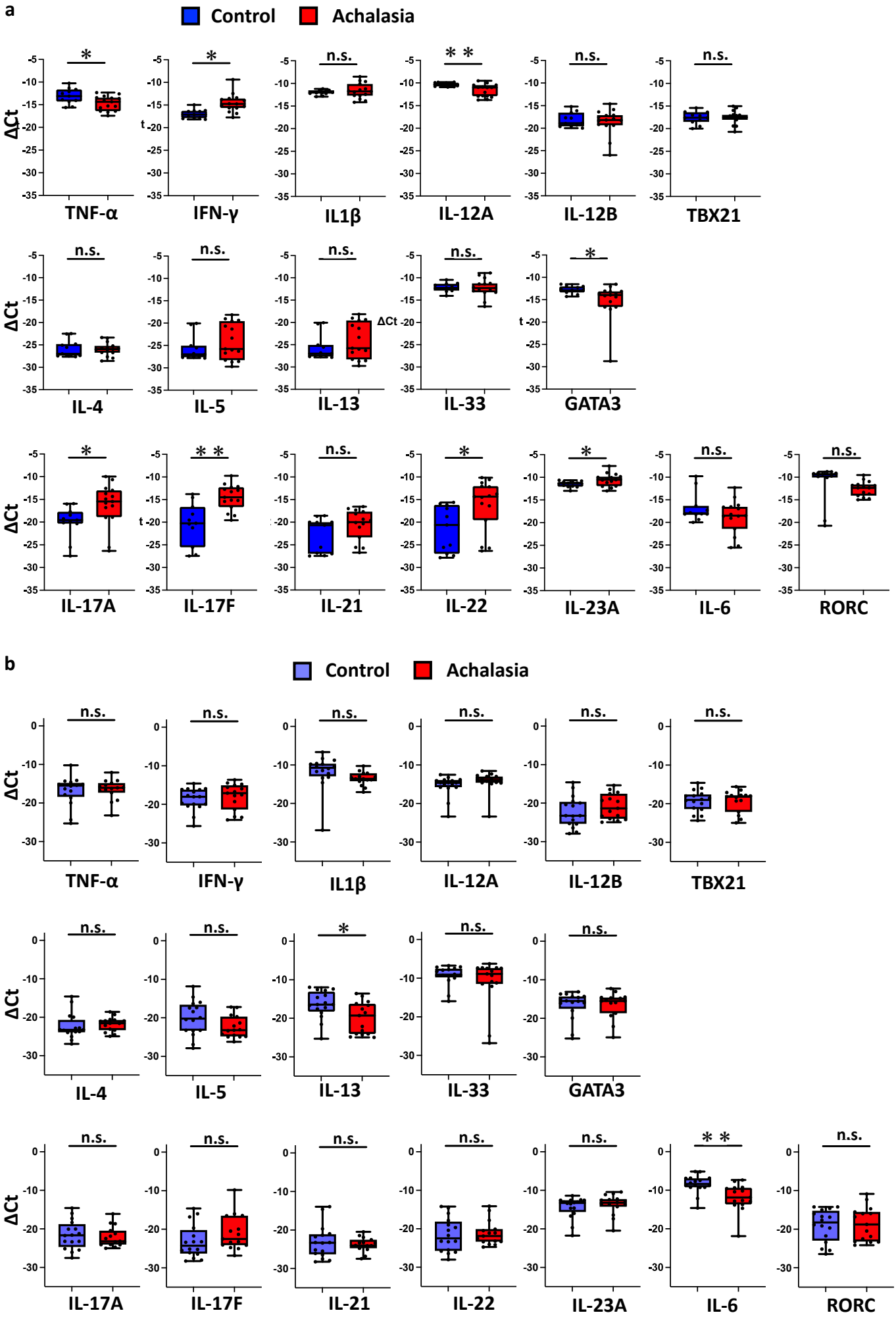
a
Control
Achalasia
ΔCt
TNF-α
IFN-γ
IL1β
IL-12A
IL-12B
TBX21
IL-4
IL-5
IL-13
IL-33
GATA3
IL-17A
IL-17F
IL-21
IL-22
IL-23A
IL-6
RORC
n.s.
*
**
b
Control
Achalasia
ΔCt
TNF-α
IFN-γ
IL1β
IL-12A
IL-12B
TBX21
IL-4
IL-5
IL-13
IL-33
GATA3
IL-17A
IL-17F
IL-21
IL-22
IL-23A
IL-6
RORC
n.s.
*
**

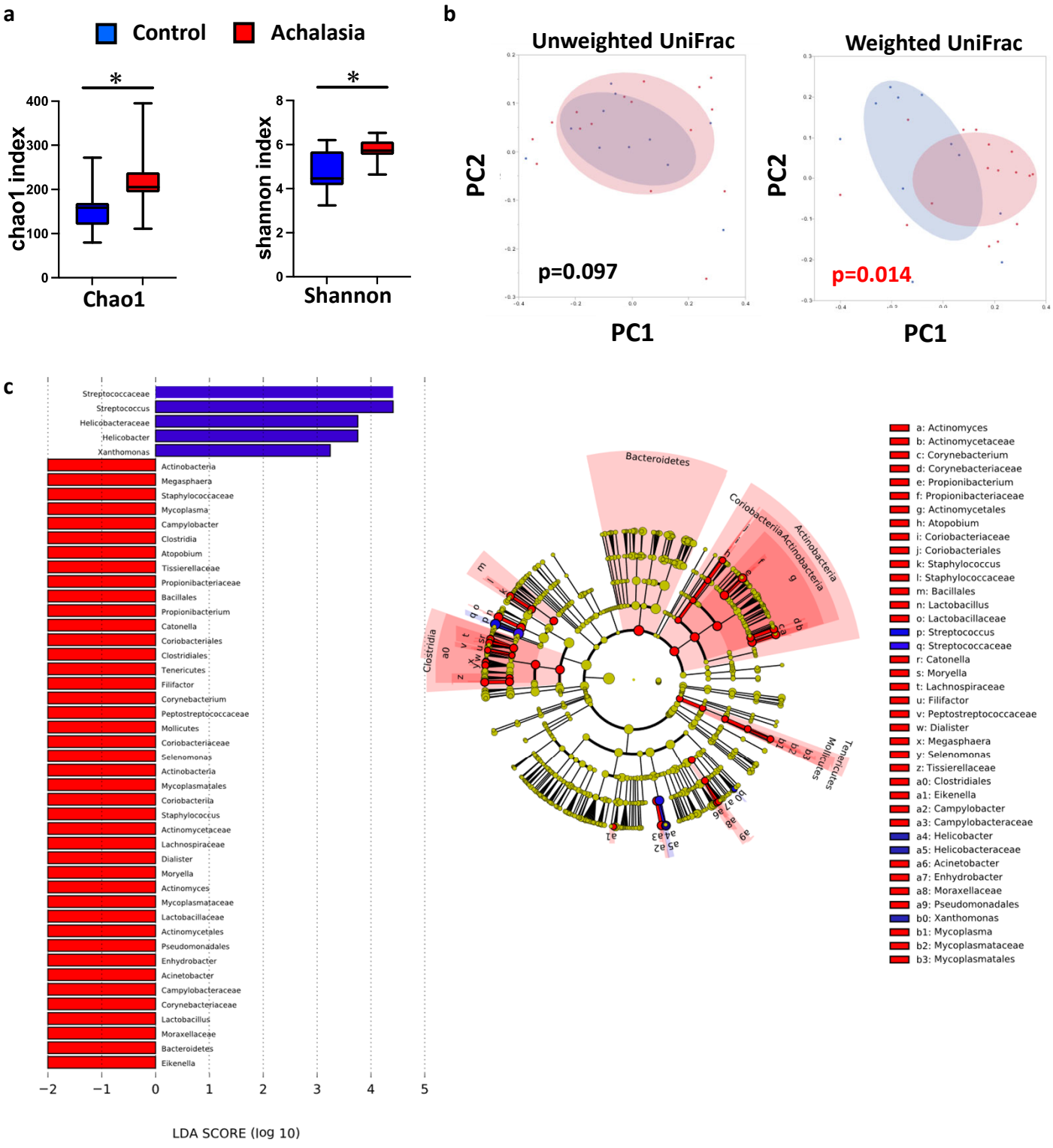
a
Control
Achalasia
chao1 index
Chao1
shannon index
Shannon
b
Unweighted UniFrac
Weighted UniFrac
PC2
PC1
p=0.097
p=0.014
c
Streptococcaceae
Streptococcus
Helicobacteraceae
Helicobacter
Xanthomonas
Actinobacteria
Megasphaera
Staphylococcaceae
Mycoplasma
Campylobacter
Clostridia
Atopobium
Tissierellaceae
Propionibacteriaceae
Bacillales
Propionibacterium
Catonella
Coriobacteriales
Clostridiales
Tenericutes
Filifactor
Corynebacterium
Peptostreptococcaceae
Mollicutes
Coriobacteriaceae
Selenomonas
Actinobacteria
Mycoplasmatales
Coriobacteriia
Staphylococcus
Actinomycetaceae
Lachnospiraceae
Dialister
Moryella
Actinomyces
Mycoplasmataceae
Lactobacillaceae
Actinomycetales
Pseudomonadales
Enhydrobacter
Acinetobacter
Campylobacteraceae
Corynebacteriaceae
Lactobacillus
Moraxellaceae
Bacteroidetes
Eikenella
LDA SCORE (log 10)
Bacteroidetes
Actinobacteria
Tenericutes
Clostridia
a: Actinomyces
b: Actinomycetaceae
c: Corynebacterium
d: Corynebacteriaceae
e: Propionibacterium
f: Propionibacteriaceae
g: Actinomycetales
h: Atopobium
i: Coriobacteriaceae
j: Coriobacteriales
k: Staphylococcus
l: Staphylococcaceae
m: Bacillales
n: Lactobacillus
o: Lactobacillaceae
p: Streptococcus
q: Streptococcaceae
r: Catonella
s: Moryella
t: Lachnospiraceae
u: Filifactor
v: Peptostreptococcaceae
w: Dialister
x: Megasphaera
y: Selenomonas
z: Tissierellaceae
a0: Clostridiales
a1: Eikenella
a2: Campylobacter
a3: Campylobacteraceae
a4: Helicobacter
a5: Helicobacteraceae
a6: Acinetobacter
a7: Enhydrobacter
a8: Moraxellaceae
a9: Pseudomonadales
b0: Xanthomonas
b1: Mycoplasma
b2: Mycoplasmataceae
b3: Mycoplasmatales
d
Esophagus

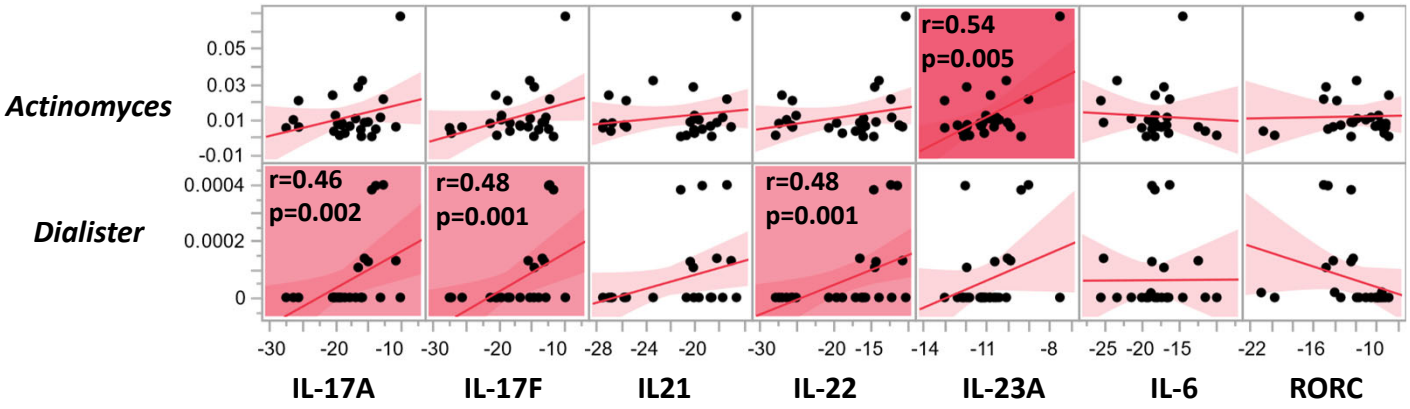
Actinomyces
Dialister
0.05
0.03
0.01
-0.01
0.0004
0.0002
0
r=0.54
p=0.005
r=0.46
p=0.002
r=0.48
p=0.001
r=0.48
p=0.001
-30 -20 -10
-30 -20 -10
-28 -24 -20
-30 -20 -15
-14 -11 -8
-25 -20 -15
-22 -16 -10
IL-17A
IL-17F
IL21
IL-22
IL-23A
IL-6
RORC

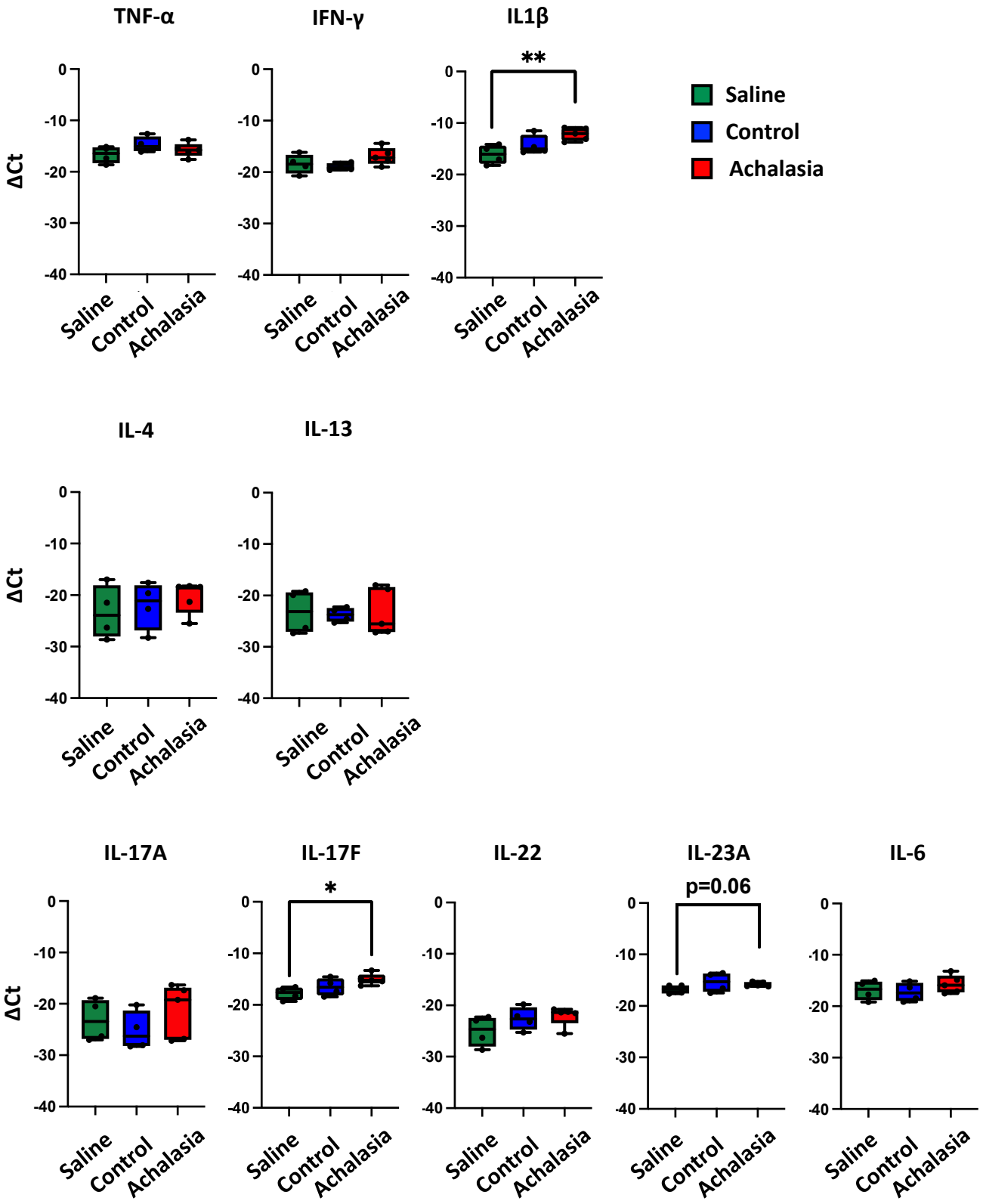
TNF-α
IFN-γ
IL1β
**
Saline
Control
Achalasia
ΔCt
0
-10
-20
-30
-40
IL-4
IL-13
IL-17A
IL-17F
*
IL-22
IL-23A
p=0.06
IL-6